CHEMISTRY
A EUROPEAN JOURNAL

DOI: 10.1002/chem.200601785

Counterion-Dependent Proton-Driven Self-Assembly of Linear Supramolecular Oligomers Based on Amino-Calix[5]arene Building Blocks

Sebastiano Pappalardo,[a] Valentina Villari,[b] Sarit Slovak,[c] Yoram Cohen,*[c] Giuseppe Gattuso,[d] Anna Notti,[d] Andrea Pappalardo,[d] Ilenia Pisagatti,[d] and Melchiorre F. Parisi*[d]

Dedicated to Professor Sir J. Fraser Stoddart on the occasion of his 65th birthday

Abstract: Self-assembly of a calix[5]arene bearing a 12-aminododecyl pendant group on the lower rim into supramolecular oligomers through intermolecular iterative inclusion events is readily triggered by contact with acid solutions and is reversed to the amino monomer precursor by treatment with a base. ^{1}H NMR data are consistent with the formation of head-to-tail assemblies derived from *endo*-cavity inclusion of the alkylammonium moiety. Diffusion NMR and light-scattering studies provide evidence for the presence of oligomers in solution and show that different counterions and concentrations result in different oligomer sizes, whereas ESI-MS and SEM investigations, respectively, indicate that self-assembly also takes place in the gas phase and in the solid state. The growth of these supramolecular oligomers is concentration-dependent; however, as a consequence of the saline nature of the monomer, it also shows a distinct counterion-dependence owing to ion-pairing/solvation effects.

Keywords: calixarenes · ion pairs · light scattering · NMR spectroscopy · supramolecular polymers

Introduction

Supramolecular polymers[1] are one of the latest developments in modern materials research. Over the past few years, a great deal of energy has been devoted to the construction of polymeric architectures, starting from simple molecules that can recognize each other and then self-assemble through weak intermolecular interactions. Several authors have focused on the use of complementary hydrogen-bonding building blocks, such as uracil derivatives and diaminopyridines,[2] cyanuric acid and melamine,[3] cyanuric acid and bis-diaminopyridines,[4] ureidopyrimidinone,[5] or even calix[4]arene tetraurea dimers,[6] to name a few representative examples. Others have investigated the possibility of using arene–arene interactions for the self-assembly of supramolecular polymers from discotic molecules, which has led to the production of a number of superstructures displaying liquid crystalline properties.[7] On the other hand, examples of supramolecular polymers obtained by exploiting iterative host–guest inclusion events are less common.[8] Relevant examples are the linear arrays of (pseudo)rotaxanes based on cyclodextrins with an apolar pendant group attached to the primary face, described by Harada et al.,[9] or the heteroditopic monomer composed of a bipyridinium moiety linked to a dibenzo[32]crown-10, reported by Gibson and co-workers.[10] In-depth studies on the formation of cyclic versus linear oligomers derived from secondary ammonium ion-substituted dibenzo[24]crown-8 have been described by the group of Stoddart.[11] Alternatively, formation

[a] Prof. S. Pappalardo
Dipartimento di Scienze Chimiche, Università di Catania
Viale A. Doria 6, 95125 Catania (Italy)

[b] Dr. V. Villari
CNR-Istituto per i Processi Chimico-Fisici
Via La Farina 237, 98100 Messina (Italy)

[c] S. Slovak, Prof. Y. Cohen
School of Chemistry, The Sackler Faculty of Exact Sciences, Tel Aviv University
Ramat Aviv 69978, Tel Aviv (Israel)
Fax: (+972) 3-640-7469
E-mail: ycohen@post.tau.ac.il

[d] Dr. G. Gattuso, Dr. A. Notti, Dr. A. Pappalardo, Dr. I. Pisagatti, Prof. M. F. Parisi
Dipartimento di Chimica Organica e Biologica, Università di Messina
Salita Sperone 31, 98166 Messina (Italy)
Fax: (+39) 090-393-895
E-mail: mparisi@unime.it

Supporting information for this article is available on the WWW under http://www.chemeurj.org/ or from the author.

of supramolecular polymers that rely on host–guest interactions has involved the use of complementary homoditopic monomers, such as bis-crown ethers and secondary diammonium ions,[12] or bis-cyclodextrin and bis-adamantyl guest molecules.[13] Within the framework of a general project aimed at the synthesis of supramolecular entities based on the calix[5]arene–primary alkylammonium ions recognition motif, we have recently described the formation of inclusion networks derived from the self-assembly of a bis-calix[5]arene receptor and long-chain α,ω-alkyldiammonium ions.[14] In this context, besides the studies on the self-assembly of the aforementioned AA/BB-type complementary homoditopic monomers, we have also been interested in the development of polymeric supramolecular structures by harnessing AB-type[15] heteroditopic monomers. Prompted by a very recent paper on the self-assembly of a pyridinium-containing calix[4]arene,[16] we now wish to report full details on the synthesis of a cone calix[5]arene derivative, bearing a long-chain alkylamino pendant group on the lower rim, and its self-assembly behavior in the presence of different acids. The self-assembly process was followed by NMR spectroscopy, diffusion NMR, static and dynamic light scattering, mass spectrometry and scanning electron microscopy. The combination of all these techniques provides conclusive evidence for the existence of self-assembled aggregates in solution, in the solid state and in the gas phase.

Results and Discussion

Synthesis of the monomer precursor 1: The target amino-calix[5]arene **1** (Scheme 1) was synthesized in three steps starting from *p-tert*-butylcalix[5]arene[17] (**2**). An excess of **2** was treated with *N*-(12-bromododecyl)phthalimide[18] to yield the phthalimidododecyloxy derivative **3** (73%), which was then exhaustively alkylated with 4-methyl-1-bromopentane to produce calix[5]arene **4** (81%). Conversion of the phthalimido moiety into an amino group by treatment with hydrazine, under standard Gabriel conditions, yielded the monomer precursor **1** (56%). Amino-calix[5]arene **1** was characterized by ^{1}H and ^{13}C NMR spectroscopy, as well as by MALDI-TOF mass spectrometry. NMR data for **1** are consistent with a C_s-symmetric structure blocked in a *cone* conformation.[19]

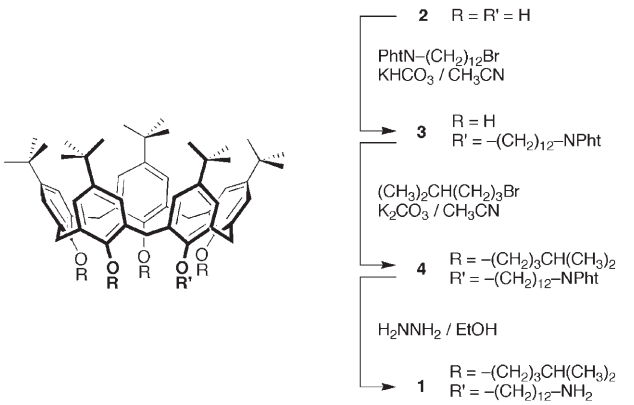

Scheme 1. Synthesis of the calix[5]arene monomer precursor **1**.

^{1}H NMR studies: Based on the known tendency of *p-tert*-butylcalix[5]arene derivatives to recognize and tightly bind unbranched primary alkylammonium ions,[20] we anticipated that simple conversion of **1** into a corresponding ammonium derivative would readily generate self-assembling monomeric species. To verify this hypothesis, a solution of amino-calixarene **1** in CD_2Cl_2 was exposed to aqueous 1 M HCl, dried ($MgSO_4$) and directly investigated by ^{1}H NMR spectroscopy. As expected, protonation of the amino group activates the self-assembly of monomer **1**·HCl, as the result of an iterative intermolecular inclusion process between the dodecylammonium moiety of one calixarene monomer and the cavity of another. This process of intermolecular complex formation/dissociation is slow on the ^{1}H NMR timescale and, accordingly, two distinct sets of resonances were observed for the end-group (unthreaded moieties)[21] and core (threaded moieties) hydrogen atoms of the resulting noncovalent oligomers $(\mathbf{1}\cdot HCl)_n$ (Figure 1). With respect to the amino precursor **1**, in CD_2Cl_2, the resonances of the oligo-

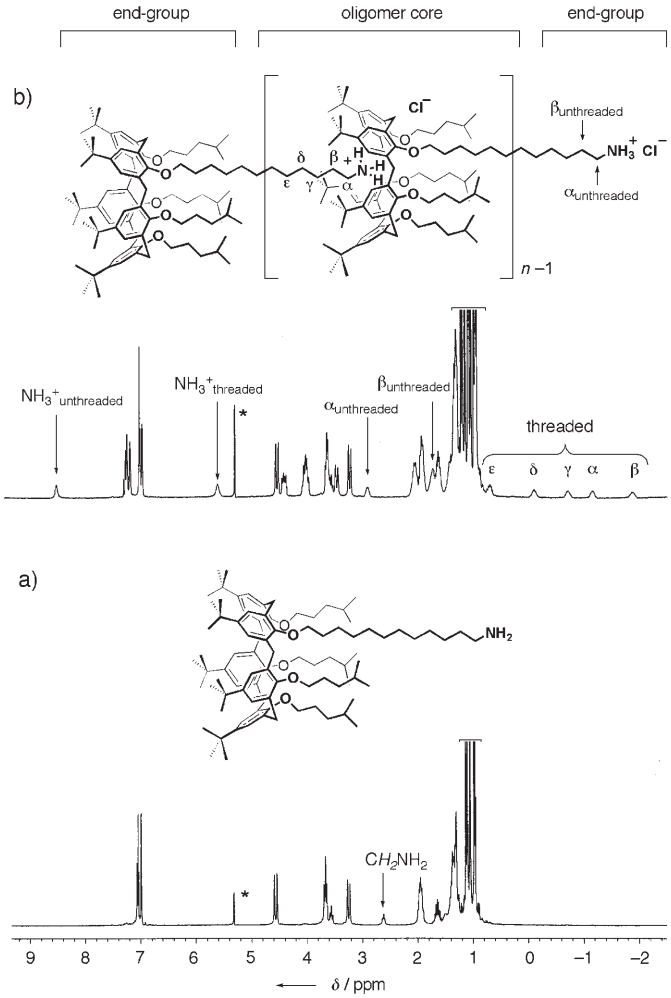

Figure 1. ^{1}H NMR spectra (300 MHz, CD_2Cl_2, 10 mM, 295 K) of: a) **1**; b) **1**·HCl. The asterisk indicates the residual solvent peak.

mer end-groups (calixarene cavity at one end and dodecylammonium moiety at the other, see Figure 1b) change very little. The most significant variations are associated with a peak ($\delta = 8.54$ ppm) for the newly formed NH_3^+ group and a downfield shift ($\Delta\delta = 0.30$ ppm) for the adjacent methylene ($CH_2NH_3^+$). On the other hand, the resonances assigned to the oligomer core undergo substantial complexation-induced shifts. Intermolecular inclusion of the dodecylammonium moiety of **1**·HCl within the cavity of another calixarene is unambiguously demonstrated by the appearance, in the high-field region ($\delta = -2.0$ to 1.0 ppm), of five peaks consistent with the methylene groups closest to the ammonium moiety (α- to ε-CH_2)[22] and by the upfield shift of the NH_3^+ resonance ($\delta = 5.63$ ppm).[23] NMR data (chemical shift as well as diffusion measurements, see below) and inspection of CPK models[24] rule out the alternative process of *endo*-cavity intramolecular inclusion (self-threading)[25] of the dodecylammonium moiety, either via the upper or the lower rim.

According to Equation (1), in the present case, the number-average degree of polymerization ($\bar{X}_n$) depends on the stability constant (K) of the interaction between the host and guest subunits of the monomers.[5,26]

$$\bar{X}_n \approx (K[\text{monomer}])^{1/2} \quad (1)$$

As mentioned above, in the case under study, formation and dissociation of the oligomers were found to be slow on the NMR time-scale, so that direct integration of key resonances (NH_3^+, ArH and α-CH_2) of both the threaded and unthreaded species (core vs end-groups) of (**1**·HCl)$_n$ were used to determine[27] the value of $\bar{X}_n$ and derive the stability constant from it by means of Equation (1) (Table 1).

One of the attractive features of noncovalent polymers over covalently bound ones is their ability to reversibly vary the degree of polymerization in response to changes in the environmental conditions. In this respect, amino-calixarene **1** is, in principle, an extremely useful precursor for polymer formation because it promptly responds to simple chemical stimuli (i.e. acid/base treatment) by activating or deactivating the self-assembly process. Calixarene **1** acts as a proton scavenger, and even trace amounts of acid present in commercial $CDCl_3$ or CD_2Cl_2 are sufficient to induce protonation and set off the self-assembly process. Similarly, the (**1**·HCl)$_n$ oligomers, in agreement with their non-covalent nature, were easily deprotonated to the free amino precursor **1** by treatment with a mild base (e.g. 1 M aqueous KOH). Furthermore, **1** could be successfully reconverted to (**1**·HCl)$_n$ upon subsequent exposure to an aqueous 1 M HCl solution, demonstrating that the oligomerization process can be controlled and turned on and off. Conversion of amino-calixarene **1** into an ammonium salt species (e.g. **1**·HCl) is a mandatory step for oligomerization/polymerization to occur. The stability constants between neutral hosts and ionic guests in low polarity media, on the other hand, are known to be influenced by ion-pairing interactions.[28] It was therefore envisaged that use of different acids would produce a variety of ammonium-calixarene salts which, as a result of the dependence of the monomer–monomer stability constant on the extent of ion-pairing, would ultimately yield oligomers of different sizes at a given monomer concentration. This hypothesis was fully confirmed by the conversion of monomer precursor **1** into (**1**·HBr)$_n$ and (**1**·HPic)$_n$ upon treatment with 1 M hydrobromic acid and 1% aqueous solution of picric acid, respectively. The end-group titration data, summarized in Table 1, indicate that in the case of **1**·HCl, a 20-fold increase in the monomer concentration hardly affects the size of the oligomers formed ($\bar{X}_n = 1.8$–1.9), whereas variations of the bromide or picrate salt monomer concentrations produce a moderate-to-marked increase of the $\bar{X}_n$ values (3–5 and 9–20 for **1**·HBr and **1**·HPic, respectively) as a consequence of a progressive loosening of the ion-pairing.

Diffusion NMR studies: Extensive diffusion NMR[29,30] experiments on CD_2Cl_2 solutions of **1**·DCl[31] and **1**·HPic unambiguously confirm intermolecular self-assembly and strongly support the formation of linear vs cyclic oligomers. In the event of intramolecular self-inclusion of the dodecylammonium moiety, the diffusion coefficient (D) of the protonated or deuterated monomers (**1**·HPic and **1**·DCl) would have remained similar to that of the amino-precursor **1**. On the contrary, diffusion data (Table 2) show that a dramatic decrease in the diffusion coefficient values follows upon protonation/deuteration of **1**. This observation is only consistent with the formation of oligomeric species (see below). Figure 2 shows stack plots of the signal decay of representative peaks of **1**, biscalix[5]arene **5**[23d] (chosen as a model compound for a species with a molecular weight roughly similar to that of the dimer of **1**), **1**·DCl and **1**·HPic as a function of the gradient strength (G) for 10 mM CD_2Cl_2 solutions at 298 K.

Stack plots (c) and (d) (see Figure 2), assigned to a pair of oligomer core peaks (i.e. cavity included α- and β-CH_2) of

Table 1. Percentages of threading for **1**·HCl, **1**·HBr and **1**·HPic and corresponding calculated number-average degree of polymerization ($\bar{X}_n$)[a] and "apparent" stability constants (K).

	[**1**·HCl] [mM]				[**1**·HBr] [mM]				[**1**·HPic] [mM]			
	2	10	25	40	2	10	25	40	2	10	25	40
% compl[b]	45	45	46	47	69	73	77	79	88	92	94	95
$\bar{X}_n$	1.8	1.8	1.9	1.9	3	4	4	5	9	13	17	20
K [M^{-1}][c]	1620	324	144	90	5120	1369	740	576	34445	15625	11156	10000

[a] For calculation of $\bar{X}_n$ values see text. [b] Determined by ^{1}H NMR (300 MHz) at 295 K in CD_2Cl_2. Values derived from the average of three independent measurements. [c] Standard error $\leq 10\%$.

Table 2. Diffusion coefficients (D) for **1**, **5**, **1**·DCl, and **1**·HPic at different concentrations in CD_2Cl_2 at 298 K.[a]

System	Peak [ppm]	D [$\times 10^{-5}$ $cm^2 s^{-1}$]			
		40 mM	25 mM	10 mM	2 mM
1	4.58	–	–	0.65 ± 0.01	–
5	4.56	–	–	0.44 ± 0.01	–
1·DCl	-1.82[b]	0.21 ± 0.01 (0.25 ± 0.01)	0.22 ± 0.01 (0.27 ± 0.01)	0.30 ± 0.01 (0.30 ± 0.01)	0.33 ± 0.01 (0.35 ± 0.01)
	4.47[b]	0.22 ± 0.01 (0.25 ± 0.01)	0.24 ± 0.01 (0.28 ± 0.01)	0.30 ± 0.01 (0.31 ± 0.01)	0.35 ± 0.01 (0.36 ± 0.01)
	4.57[c]	0.23 ± 0.01 (0.26 ± 0.01)	0.25 ± 0.01 (0.29 ± 0.01)	0.31 ± 0.01 (0.32 ± 0.01)	0.36 ± 0.01 (0.36 ± 0.01)
	7.02[c]	0.23 ± 0.01 (0.27 ± 0.01)	0.25 ± 0.01 (0.29 ± 0.01)	0.31 ± 0.01 (0.32 ± 0.01)	0.36 ± 0.01 (0.37 ± 0.01)
	7.30[b]	0.21 ± 0.01 (0.25 ± 0.01)	0.23 ± 0.01 (0.27 ± 0.01)	0.29 ± 0.01 (0.30 ± 0.01)	0.34 ± 0.01 (0.35 ± 0.01)
1·HPic	-1.82[b]	0.07 ± 0.01	0.10 ± 0.01	0.15 ± 0.01	0.27 ± 0.01
	4.47[b]	0.07 ± 0.01	0.10 ± 0.01	0.15 ± 0.01	0.27 ± 0.01
	4.61[c]	0.11 ± 0.01	0.13 ± 0.01	0.18 ± 0.01	0.31 ± 0.01
	7.02[c]	0.10 ± 0.01	0.13 ± 0.01	0.19 ± 0.01	0.30 ± 0.01
	7.30[b]	0.07 ± 0.01	0.09 ± 0.01	0.15 ± 0.01	0.26 ± 0.01
	8.93[d]	0.64 ± 0.01	0.62 ± 0.01	0.57 ± 0.01	0.64 ± 0.01

[a] Diffusion experiments were performed in triplicate and the reported values are the mean ± standard deviation of the mean. Values for **1**·DCl refer to CD_2Cl_2 solutions containing 1.33% of DCl/D_2O (see ref. [31]), corresponding values for D_2O-free CD_2Cl_2 solutions (see ref. [35]) are reported in parentheses. [b] Peak assigned to the core of the oligomers. [c] Peak assigned to the end-groups of the oligomers. [d] Peak assigned to the picrate anion.

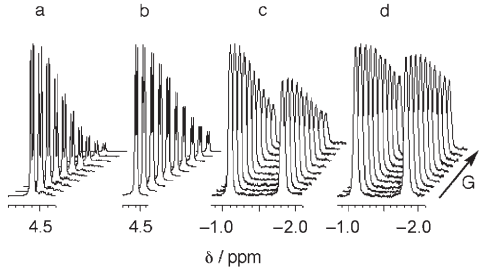

Figure 2. ^{1}H NMR stack plots of the signal decay (CD_2Cl_2, 10 mM, 298 K) as a function of the gradient strength (G) of a) **1**, b) **5**, c) **1**·DCl and d) **1**·HPic.

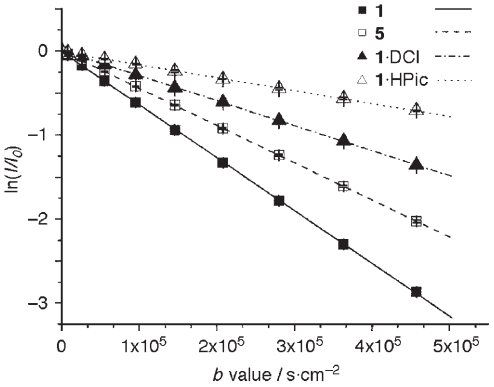

Figure 3. Plot of the natural logarithm of the normalized signal decay ($\ln I/I_0$) of the peaks shown in Figure 2, as a function of the b values for 10 mM CD_2Cl_2 solutions of **1**, **5**, **1**·DCl and **1**·HPic at 298 K.

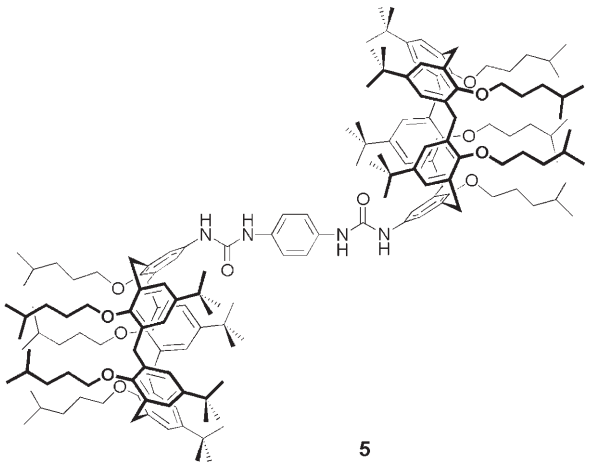

1·DCl and **1**·HPic, respectively, clearly show that their signals decay much more slowly compared to those of stack plots (a) and (b) pertaining to the ArCH_2Ar peaks of **1** and **5**. Figure 3 shows the plot of the natural logarithm of the normalized signal decay $\ln I/I_0$ as a function of the diffusion weighting b values (see the Experimental Section for details) for the peaks shown in Figure 2 from which the diffusion coefficients were extracted.

The data in Table 2 show that, at any given concentration, both **1**·DCl and **1**·HPic always have much lower diffusion coefficients than **1** or even the model biscalixarene **5**. These observations are consistent with the formation of non-covalent oligomers (i.e. $(\mathbf{1}\cdot DCl)_n$ and $(\mathbf{1}\cdot HPic)_n$) in the case of **1**·DCl and **1**·HPic. It is also clear from the smaller D values measured for **1**·HPic over **1**·DCl that the former generates larger aggregates. Diffusion NMR provides a means to simultaneously obtain the diffusion coefficients of all the different supramolecular species co-existing in solution, as long as they display distinct and not superimposed peaks. As mentioned above, two distinct sets of ^{1}H NMR peaks were found for the end-groups and core of oligomers $(\mathbf{1}\cdot DCl)_n$ and $(\mathbf{1}\cdot HPic)_n$. Figure 4 shows the stack plots of the signal decay as a function of the gradient strength (G) for the ArCH_2Ar peaks assigned to the end-groups (traces 4a, c) and core (traces 4b, d) of the oligomers derived from **1**·DCl and **1**·HPic (traces 4a, b and 4c, d, respectively). Figure 5 shows the plot of the natural logarithm of the normalized signal decay as a function of the b values for the peaks shown in Figure 4. Interestingly, we found different diffusion

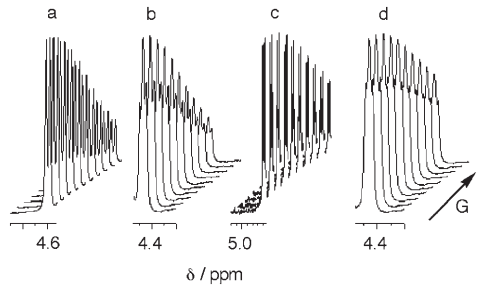

Figure 4. ^{1}H NMR stack plots of the signal decay (CD_2Cl_2, 10 mM, 298 K) as a function of the gradient strength (G) of a) **1**·DCl oligomer end-group, b) **1**·DCl oligomer core, c) **1**·HPic oligomer end-group and d) **1**·HPic oligomer core.

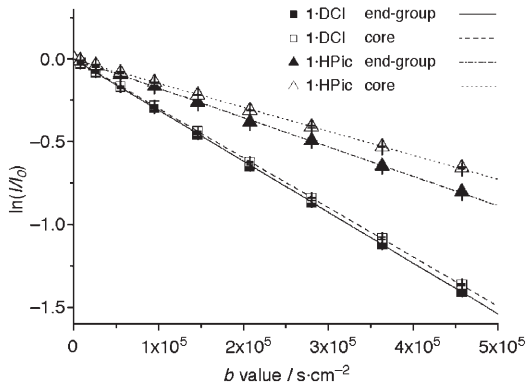

Figure 5. Plot of the natural logarithm of the normalized signal decay ($\ln I/I_0$) as a function of the b values for the peaks representing the end-group and core of the oligomers of **1**·DCl and **1**·HPic in 10 mM CD_2Cl_2 solutions.

coefficients for the two sets of peaks that were assigned to the end-groups and core of these oligomers, the D values of the former being always higher than those of the core (Table 2). The most plausible explanation for these findings is that core and end-group units are in slow exchange with each other, while the latter are, in turn, rapidly exchanging with the fraction of free monomer present in solution. Because it is reasonable to assume that the diffusion coefficients of monomers **1**·DCl and **1**·HPic are as high as that of the monomer precursor **1**, it was therefore concluded that the D values referring to the oligomer end-groups express a weighted average of the diffusion coefficients of the free monomer and the oligomers present in solution at a given concentration. By the same token, the different diffusion coefficients measured for the two sets of peaks (core versus end-groups) of both $(\mathbf{1}\cdot\mathrm{DCl})_n$ and $(\mathbf{1}\cdot\mathrm{HPic})_n$ corroborate, at the same time, the formation of linear rather than cyclic oligomers.

Assuming cyclic oligomers[32] were formed in a preponderant amount, for a cyclic aggregate one should expect to find only one set of peaks characterized by a single averaged value of the diffusion coefficient. This is clearly not the case here (Table 2): the D values found for the unthreaded set of calixarene peaks (e.g. ArCH_2Ar at $\delta = 4.57$ and 4.61 ppm for **1**·DCl and **1**·HPic, respectively) are far too low to be compatible with that of the monomer (or its unprotonated precursor **1**, $\delta = 4.61$ ppm). The diffusion coefficients, extracted from the plots of $\ln I/I_0$ versus b values (Figure 6), unambiguously indicate that the size of the non-covalent oligomers formed from **1**·DCl and **1**·HPic is both concentration- and anion-dependent. Data from Table 2 were also conveniently used to calculate the average number of monomer units present in the oligomers by means of a recent hydrodynamic model[33] that takes into account the effect of the number of repeating units on the diffusion coefficient of a cylindrical molecular assembly. According to this model, the number-average degree of polymerization was found to be 5, 6, and 10 for **1**·DCl and 8, 20, and 36 for **1**·HPic when the concentrations were 2, 10, and 25 mM, respectively.

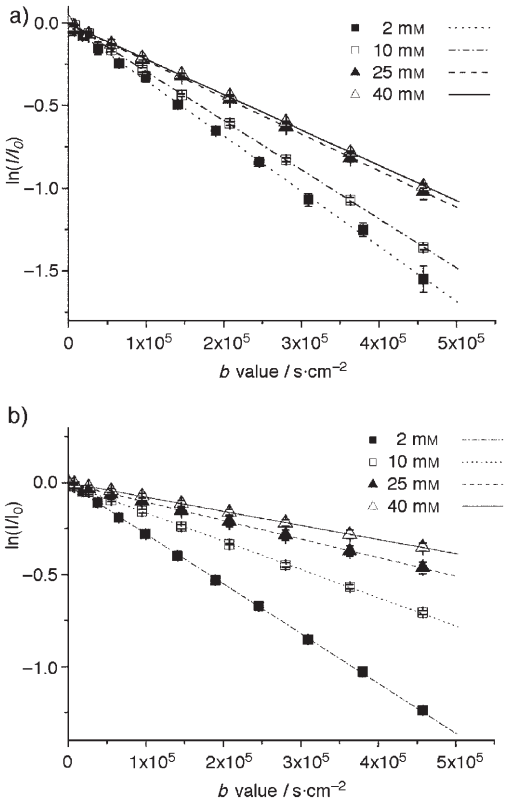

Figure 6. Plot of the natural logarithm of the normalized signal decay ($\ln I/I_0$) (298 K, CD_2Cl_2) as a function of the b values for the peaks representing the oligomer core at different concentrations a) **1**·DCl and b) **1**·HPic.

The $\bar{X}_n$ values determined in this way, together with those obtained by end-group titration (although in some cases quite different, see Table 1) provide qualitative clear-cut evidence of the crucial role played by the calixarene counterion. From these data, it is evident that non-covalent oligomers derived from **1**·HCl and **1**·DCl are, at any given concentration, smaller than those obtained from **1**·HPic. The two sets of $\bar{X}_n$ values obtained for the latter compare better at lower concentrations (e.g. 2 mM) because the ^{1}H NMR in-

tegral accuracy is more reliable, being closer to the useful 20–80% range.[34]

Besides, it should also be mentioned that—in the case of the diffusion data—viscosity effects cannot be ruled out for CD_2Cl_2 solutions at 25 mM or higher concentrations, and as a consequence an overestimation of the $\bar{X}_n$ values is also likely. The discrepancy observed between **1**·HCl and **1**·DCl data, on the other hand, deserves comment. These differences in the degree of polymerization obtained by ^{1}H NMR integration and diffusion NMR data can be attributed, to some extent, to the different preparation procedures of the samples or to some self-aggregation of the charged oligomeric chains formed in the CD_2Cl_2 solution. Self-aggregation between chains, which would result in a decrease in the observed diffusion coefficients and in an overestimation of the average aggregation number ($\bar{X}_n$), would be concentration-dependent and much more significant at high concentrations. It should be remembered that **1**·DCl samples, obtained in situ by DCl/D_2O addition to a CD_2Cl_2 solution of **1**,[31] inevitably undergo ion solvation and the extent of ion-pairing varies as a result (see below).[35] In addition, one should also bear in mind that the end-group integration includes a contribution from the monomer present in the solution.

It is worth noticing that, in agreement with the Hofmeister trend,[36] the increasing efficiency of the self-assembly processes can be correlated to the decreasing intensity of ion-pairing interactions between the ammonium monomer **1**·H^+ and its counterion ($Pic^- < Br^- < Cl^-$).[28] This trend is reflected in a qualitative fashion by the chemical shifts of the uncomplexed ammonium end-group ($\delta = 8.54$, 8.13, and 7.87 ppm for **1**·HCl, **1**·HBr and **1**·HPic, respectively), which show that the tighter the ion pair, the higher the deshielding observed on this resonance, and by the much lower diffusion coefficient of **1**·HPic compared to that of **1**·DCl at a given concentration. Indeed, the diffusion coefficients listed in Table 2 clearly demonstrate that the picrate anion is not ion-paired to the oligomer.[37] The diffusion coefficient for this counterion ($\delta = 8.93$ ppm) is concentration-independent and its value is close to that of simple alkylammonium salts (e.g. hexylammonium picrate) and in comparison much higher than the one measured for the oligomers present in the same CD_2Cl_2 solution. On the one hand, our findings suggest that the degree of polymerization can, to some extent, be modulated by changing the calixarene counterion in the initial protonation step leading to the formation of the monomer salt. On the other hand, a closer look at the data reported in Tables 1 and 2 reveals that unavoidable ion-pairing effects, intrinsic to saline monomers in apolar solvents, are responsible for reducing the self-assembly efficiency of these systems at high concentration. For a given monomer, on going from a lower to a higher concentration, the number-average degree of polymerization does not increase as fast as would be expected on the basis of Equation (1) as a result of a parallel decrease in the K value. This dependence of the "apparent" K values on the concentration is consistent with the monomers being ion-paired while their corresponding oligomers are not. If both monomers and oligomers were ion-paired no such trend would be observed, although each salt would behave differently. In our cases the "active" monomeric species undergoing oligomerization is the cation rather than the ion-paired salt, and consequently the latter has to dissociate prior to self-assembly. As a result of this, comparatively more efficient self-assembly processes (higher "apparent" K values[28d]) take place at lower monomer concentrations (i.e. 2 mM), where the extent of salt dissociation is higher.

Light-scattering studies: To gain further evidence of oligomer formation in solution and obtain at the same time an independent evaluation of their (average) size and mass, both static and dynamic light scattering (SLS and DLS) measurements[38] were carried out. The SLS technique is able to measure the absolute molecular weight of a macromolecule by making use of the time-averaged intensity of the scattered light as a function of the sample concentration. Accordingly, from the scattered intensity at 90° of a 10 mM CH_2Cl_2 solution of **1**·HPic, an intensity-weighted average aggregation number of approximately 17 was calculated, using the Rayleigh expression (see the Experimental Section). Interestingly, this value is in good agreement with that determined at the same concentration by diffusion NMR ($\bar{X}_n = 20$). An insight into the oligomer-size distribution in solution came from DLS[39] data, which indicate the presence of two families of aggregates having hydrodynamic radii (R_H) of about 2 and 35 nm, respectively (Figure 7). From the spectral contribution of both aggregates to the correlation function, after an appropriate correction for the scattering efficiency, it emerges that the smaller aggregates are predominant, but about 0.04% of the total mass of (**1**·HPic)$_n$ is assembled in larger aggregates. Assuming that the mass of the aggregates is homogeneously distributed,[40] the aggregation numbers were estimated to be 6 and 30000 for $R_H = 2$ and $R_H = 35$ nm, respectively. In the case of a 10 mM CH_2Cl_2 so-

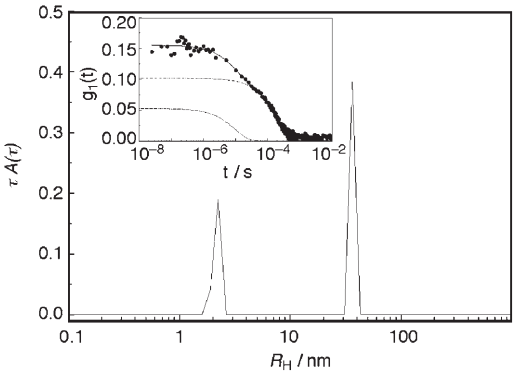

Figure 7. Size distribution of **1**·HPic oligomers obtained by multi-exponential non-negative least-square fit (NNLS). Inset: the scattered electric field correlation function ($g_1(t)$) is reported together with the NNLS fit (continuous line). Dashed and dotted lines represent the main components of the distribution.

lution of **1**·HBr, a similar DLS investigation revealed the presence of only one type of aggregate with $R_H \cong 1.5$ nm and an aggregation number of ≅5.

ESI-MS and SEM studies: Electron-spray ionization mass spectroscopy (ESI-MS)[41] investigations (Figure 8) on a

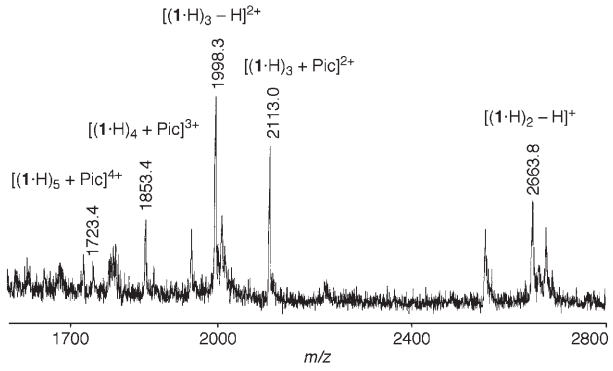

Figure 8. Section of the ESI-MS spectrum of a 0.5 mM sample solution of **1**·HPic in CH_2Cl_2/CH_3OH (5:4, v/v).

0.5 mM sample solution of **1**·HPic in CH_2Cl_2/CH_3OH (5:4, v/v) show the presence of a prominent peak at *m*/*z* 1332.1 corresponding to $[\mathbf{1}\cdot H]^+$ (base peak), along with a diagnostically important series of multi-charged ion peaks of much lower intensity (≤5%) at *m*/*z* 2113.0, 1853.4, and 1723.4 corresponding to the general formulation $[(\mathbf{1}\cdot H)_n + Pic]^{(n-1)+}$ ($n = 3, 4, 5$). The latter demonstrate the existence of oligomeric fragments—containing up to five monomer units—also in the gas phase.

In addition to the solution studies discussed above, a scanning electron microscopy (SEM) analysis of gold-coated fibers, obtained by slow evaporation of a 10 mM chloroform solution of **1**·HPic, provided direct evidence of the formation of supramolecular assemblies of nanoscopic dimensions in the solid state. The secondary electron SEM images (Figure 9) show a quite uniform material, having a typical interwoven fibrous morphology with individual fibers up to 100 μm long and about 800 nm wide.

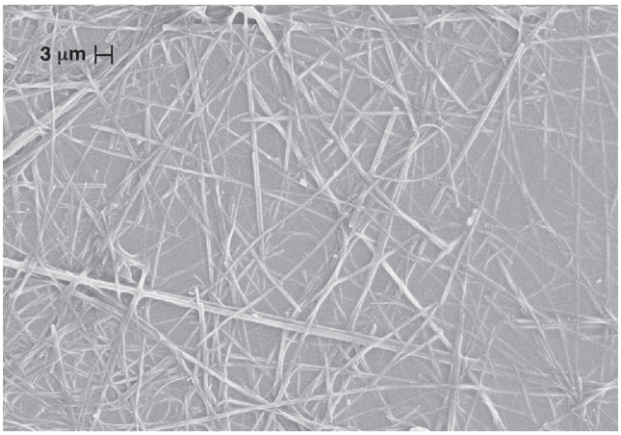

Figure 9. Scanning electron micrograph of (gold-coated) fibers formed by slow evaporation of a 10 mM solution of **1**·HPic in $CHCl_3$. Magnification: 2990×.

Conclusion

In conclusion, we have shown that a calix[5]arene bearing an alkylamino pendant group of an appropriate length is able to form, upon protonation, supramolecular oligomers as a result of iterative intermolecular inclusion processes. With this type of molecule, oligomer formation or reversal to the original monomer precursor can be controlled (on and off switching) by means of simple acid/base treatment and, since oligomerization is influenced by ion-pairing effects between the cationic monomer and its counterion, the oligomer size can be tuned, to some extent, via the formation of a variety of monomeric salt species (exposure to different acids). The self-assembly of calixarene monomers **1**·HX in solution has been investigated by a number of techniques (^{1}H and diffusion NMR, SLS, DLS), which in combination have provided conclusive evidence on the formation of linear head-to-tail oligomers, whose size is both concentration- and counterion-dependent. Oligomeric assemblies have also been detected in the gas phase (ESI-MS) and additionally confirmed in the solid state by SEM (fibrous structures were observed upon solvent evaporation).

We believe that these studies provide the basis for the future design of linear supramolecular polymers based on heteroditopic salt monomers. The drawback represented by ion-pairing effects on the growth of such polymers calls for the synthesis of new heteroditopic compounds that will also incorporate an auxiliary counterion binding site in their structure. It is likely that such an additional structural feature would facilitate salt dissociation (by overriding ion-pair interactions) and ultimately make polymer formation more efficient. The strategy of harnessing non-covalent host–guest interactions between building blocks derived from pH-sensitive calixarene monomer precursors—equipped with an additional anion recognition site—for the construction of new supramolecular polymers as novel "daptive materials"[1c] is currently under investigation.

Experimental Section

General: Melting points were determined on a Kofler hot stage apparatus and are uncorrected. Unless otherwise stated, ^{1}H and ^{13}C NMR spectra were recorded at 295 K in $CDCl_3$, at 300 and 75 MHz respectively, using TMS as an internal standard. CH_3CN was dried by standard methods,[42] HCl-free $CHCl_3$ and $CDCl_3$, employed for the synthesis and the NMR analysis of **1**, were passed through neutral alumina prior to use; all other chemicals were reagent grade and were used without further purification. Column chromatography was performed on silica gel (Merck; 230–400 mesh). All reactions were carried out under an argon atmosphere. *p-tert*-Butylcalix[5]arene **2**[17] and bis-calix[5]arene **5**[23d] were synthesized according to a literature procedure.

Diffusion NMR spectroscopy: Diffusion NMR experiments were carried out on a 400 MHz NMR spectrometer equipped with a z-gradient system

capable of producing a maximal pulse gradient of about 50 gauss cm^{-1}. These NMR diffusion experiments were performed with a conventional 5-mm inverse probe and a longitudinal eddy currents (LED) sequence[43] with a sine-shaped gradient pulse. For the diffusion measurements, the samples were placed in 4 mm NMR tubes that were then placed coaxially in 5-mm NMR tubes. The diffusion coefficients were extracted from Equation (2):

$$\ln I/I_0 = -\gamma^2\delta^2G^2(2/\pi)^2(\Delta-\delta/4)\,D = -b\,D \qquad (2)$$

where I and I_0 are the echo intensity, in the presence and absence of the gradient pulse, respectively, γ is the gyromagnetic ratio, G is the pulse gradient strength, $2/\pi$ is a geometrical correction factor due to the sine-shape of the pulse gradients used, δ is the length of the pulse gradient, Δ is the time interval between the leading edges of the pulse gradient used, and D is the diffusion coefficient. The diffusion coefficients were extracted from the slope of the plot of $\ln I/I_0$ versus the b value. All diffusion NMR data were acquired at 298 K and were obtained in triplicate. The given values are means ± the standard deviation of the means. Only data for which correlation coefficients were higher than 0.999 were considered.

Light scattering: Static and dynamic light scattering (SLS) and (DLS) measurements were carried out using a 200-mW polarized laser source Nd:YAG ($\lambda = 532$ nm). The polarized scattered light was collected at 90° in a self-beating mode with a Hamamatsu R942/02 photomultiplier. The signal was sent to a Malvern 4700 submicrometer particle analyser system to measure the intensity autocorrelation function. CH_2Cl_2 used for the preparation of the **1**·HPic and **1**·HBr solutions (10 mM) was filtered, prior to use, through a Teflon filter (pore size 0.45 μm). Refractive index (n = 1.425) for CH_2Cl_2 and refractive index increment ($dn/dc = (0.135 \pm 0.005)$ cm^3 g^{-1}) for the CH_2Cl_2 solutions of **1**·HPic and **1**·HBr, required for the aggregation number determination, were measured with a home-made deflection-type refractometer, calibrated with a NaCl solution.

SLS: The scattered intensity at 90° ($I_{90°}$), subtracted for the contribution from the solvent and normalized by the scattered intensity of toluene, was used to determine the aggregation number of Rayleigh scatterers [Eq. (3)]:[38]

$$I_{90°} = NKM_w c \qquad (3)$$

where N is the aggregation number, M_w is the molecular weight of the calixarene monomer, c is the mass concentration and $K = (4\pi^2n^2)/(\lambda^4 N_A)(dn/dc)^2$ is the optical constant (n is the refractive index of the solvent, dn/dc is the refractive index increment of the solution, λ is the wavelength in a vacuum and N_A is the Avogadro number).

DLS: The intensity autocorrelation function ($g_2(t)$) containing the information on the diffusion coefficient D of monodisperse scatterers by means of the scattered electric field correlation function $g_1(t)$ [Eq. (4)]:[39]

$$g_1(t) \propto [g_2(t)-1]^{1/2} = \exp(-t/\tau) \qquad (4)$$

where $\tau = 1/(Dq^2)$ and q is the exchanged momentum of the scattered light. The hydrodynamic radius (R_H), was calculated with the Einstein–Stokes relation [Eq. (5)]:[38]

$$R_H = (K_B T)/(6\pi\eta D) \qquad (5)$$

where η is the solvent viscosity, T is the temperature, and K_B is the Boltzmann constant. In the case of a polydisperse sample, the correlation function is a superposition of exponential functions with different decay rates.

$$g_1(t) = \int \tau A(\tau)\exp(-t/\tau)d(\ln\tau) \qquad (6)$$

The distribution of these decay rates can be obtained through a Laplace inversion of the field correlation function $g_1(t)$.[39,44] A discrete multi-exponential non-negative least-squares fit (NNLS)[45] was used to perform this inversion procedure.

Mass spectrometry: Matrix-assisted laser desorption-time (MALDI-TOF) mass spectra were recorded in the reflector mode on a Voyager STR instrument (Applied Biosystems, Framingham, MA, USA) equipped with a nitrogen laser ($\lambda = 337$ nm) and provided with delayed extraction technology. Ions formed by the pulsed laser beam were accelerated through 24 kV. Each spectrum is the result of approximately 200 laser shots. External calibration was applied, calibration was about 12000 (FWHM). 2,5-Dihydroxybenzoic acid (DHB) was used as the matrix. Electron-spray ionization (ESI) mass spectra were recorded on a Finnigan LCQDECA ThermoQuest mass spectrometer with the following main settings: source voltage, 5 V; capillary voltage, 40 V; capillary temperature, 225 °C; standard calibration. Sample solutions were introduced into the mass spectrometer source with a syringe pump at a flow-rate of 5 μL min^{-1}. The final spectrum is the sum of several scans.

Scanning electron microscopy: Investigations were carried out on a LEO S420 instrument operating at an energy of 10 keV, an I probe of 9 pA and a working distance of 9 mm. All observations were performed from low to higher magnifications up to ≈45000×.

***N*-(12-Bromododecyl)phthalimide**:[18] Potassium phthalimide (0.93 g, 5.0 mmol) and 1,12-dibromododecane (4.9 g, 15.0 mmol) were stirred at 180 °C for 16 h. The reaction mixture was cooled, diluted with chloroform, filtered and the filtrate was evaporated to dryness. Unreacted potassium phthalimide was filtered off after sonication with petroleum ether. The crude product obtained after solvent evaporation was purified by column chromatography (SiO_2, petroleum ether/AcOEt 95:5) followed by recrystallization from petroleum ether to yield pure *N*-(12-bromododecyl)phthalimide (1.0 g, 51 %). M.p. 59–61 °C (petroleum ether, lit.:[18] 62–63 °C). ^{1}H NMR spectral data were in agreement with those reported in the literature.[18]

31-[12-*N*-(Phthalimidododecyl)oxy]-32,33,34,35-tetrahydroxy-5,11,17,23,29-penta-*tert*-butylcalix[5]arene (3): A stirred mixture of **2** (1.16 g, 1.43 mmol), *N*-(12-bromododecyl)phthalimide (0.2 g, 0.5 mmol) and $KHCO_3$ (0.29 g, 2.9 mmol) in anhydrous CH_3CN (40 mL) was refluxed for 42 h. The solvent was evaporated under reduced pressure, and the residue was partitioned between chloroform and aqueous HCl (0.1 M). The organic layer was dried (Na_2SO_4) and concentrated. The crude product was purified by column chromatography (SiO_2, petroleum ether/Et_2O 95:5 to remove the excess of **2**, then $CHCl_3$) to give **3** (410 mg, 73 %). M.p. 107–109 °C; ^{1}H NMR: δ = 1.09, 1.23, 1.29 (s, 1:2:2, 45H, C(CH_3)$_3$), 1.27–1.54 (m, 14H), 1.57–1.71 (m, 4H), 2.01–2.13 (m, 2H), 3.43 and 4.35 (AX system, J = 13.8 Hz, 4H, ArCH_2Ar), 3.46 and 4.15 (AX system, J = 14.2 Hz, 4H, ArCH_2Ar), 3.48 and 4.07 (AX system, J = 14.5 Hz, 2H, ArCH_2Ar), 3.66 (t, J = 7.3 Hz, 2H, NCH_2), 4.09 (t, J = 6.8 Hz, 2H, OCH_2), 7.12 (s, 2H, *Ar*), 7.16 and 7.19 (AB system, J = 2.4 Hz, 4H, *Ar*), 7.20 (s, 4H, *Ar*), 7.66–7.73 and 7.79–7.85 (AA′BB′ system, 4H, *Pht*), 7.87 and 7.95 ppm (br s ×2, 4H, O*H*); ^{13}C NMR: δ = 26.0, 26.9, 28.6, 29.2, 29.49, 29.53, 29.57, 29.59, 29.62, 30.0, 30.6, 31.2, 31.3, 31.4, 31.5, 31.7, 33.8, 34.1, 38.1, 75.9, 123.1, 125.4, 125.5, 125.6, 125.8, 126.0, 126.37, 126.39, 126.5, 126.9, 132.1, 132.2, 133.8, 142.6, 143.8, 147.2, 147.6, 149.2, 150.3, 168.5 ppm; MALDI-TOF MS: m/z: 1146.7 [M+Na]$^+$, 1162.7 [M+K]$^+$; elemental analysis calcd (%) for $C_{75}H_{97}NO_7$: C 80.10, H 8.69, N 1.25; found: C 80.34, H 8.81, N 1.22.

31-[12-*N*-(Phthalimidododecyl)oxy]-32,33,34,35-tetra-(4-methyl-pentyl-oxy)-5,11,17,23,29-penta-*tert*-butylcalix[5]arene (4): Calix[5]arene **3** (380 mg, 0.34 mmol), 1-bromo-4-methylpentane (677 mg, 4.1 mmol) and K_2CO_3 (560 mg, 4.1 mmol) were suspended in anhydrous CH_3CN (50 mL) and refluxed for 16 h, under a vigorous stirring. Inorganic salts were filtered off and washed with $CHCl_3$. The combined filtrates were evaporated to dryness under reduced pressure, and the residue was triturated with MeOH to give **4** (400 mg, 81 %). M.p. 124–126 °C; ^{1}H NMR: δ = 0.95 (d, J = 6.6 Hz, 24H, CH(CH_3)$_2$), 1.01, 1.06, 1.09 (s, 2:2:1, 45H, C(CH_3)$_3$), 1.26–1.50 (m, 22H), 1.55–1.72 (m, 8H), 1.84–1.95 (m, 10H), 3.25 and 4.55 (AX system, J = 13.8 Hz, 10H, ArCH_2Ar), 3.56 (t, J = 7.0 Hz, 2H, OCH_2C$_{11}$H$_{22}$), 3.65 (t, J = 7.3 Hz, 8H, OCH_2CH$_2$CH$_2$CH(CH$_3$)$_2$), 3.69 (t, J = 7.2 Hz, 2H, NCH_2), 6.90, 6.94, 6.97 (s, 2:2:1, 10H, *Ar*), 7.66–7.74 and 7.81–7.88 ppm (AA′BB′ system, 4H, *Pht*); ^{13}C NMR: δ = 22.8, 26.3, 26.9, 28.3, 28.4, 28.6, 29.26, 29.33, 29.4, 29.6, 29.7, 29.8, 30.1, 30.2, 30.6, 31.4, 31.41, 31.44, 33.92, 33.94, 33.95, 35.1, 35.2, 38.1, 73.9, 74.3 (×2),

123.1, 125.2, 125.3, 125.4, 125.5, 132.2, 133.76, 133.78, 133.91, 133.93, 144.4, 152.7, 152.8, 168.5 ppm; MALDI-TOF MS: m/z: 1483.1 $[M+Na]^+$; elemental analysis calcd (%) for $C_{99}H_{145}NO_7$: C 81.38, H 10.00, N 0.96; found: C 81.77, H 10.19, N 0.94.

31-[(12-Aminododecyl)oxy]-32,33,34,35-tetra-(4-methylpentyloxy)-5,11,17,23,29-penta-*tert*-butylcalix[5]arene (1): A stirred mixture of calix[5]arene **4** (330 mg, 0.158 mmol) and hydrazine monohydrate (84 μL, 1.72 mmol) in EtOH (20 mL) was refluxed for 3 h. The solvent was evaporated under reduced pressure. The residue was dissolved in $CHCl_3$, washed with aqueous NaOH (5% w/w), dried (Na_2SO_4), and the solution was evaporated to dryness. Crystallization of the residue from CH_3CN/$CHCl_3$ afforded **1** (118 mg, 56%). M.p. 55–57 °C; ^{1}H NMR: $\delta = 0.94$ (d, $J = 6.6$ Hz, 24H, $CH(CH_3)_2$), 1.00, 1.05, 1.08 (s, 2:2:1, 45H, $C(CH_3)_3$), 1.10–1.48 (m, 22H), 1.52–1.68 (m, 8H), 1.82–1.95 (m, 10H), 2.68 (t, $J = 6.9$ Hz, 2H, NCH_2), 3.24 and 4.54 (AX system, $J = 13.8$ Hz, 10H, $ArCH_2Ar$), 3.54 (t, $J = 7.0$ Hz, 2H, $OCH_2C_{11}H_{22}$), 3.64 (t, $J = 7.3$ Hz, 8H, $OCH_2CH_2CH_2CH(CH_3)_2$), 6.88, 6.93, 6.96 ppm (s, 2:2:1, 10H, *Ar*) (NH_2 protons not detected); ^{13}C NMR: $\delta = 22.8$, 28.3, 28.4, 29.37, 29.43, 29.6, 29.7, 29.8, 30.1, 30.2, 30.6, 31.38, 31.42, 34.0, 35.1, 35.2, 73.9, 74.3, 125.2, 125.37, 125.42, 125.5, 133.8, 133.9, 134.0, 144.5, 152.7, 152.8 ppm; MALDI-TOF MS: m/z: 1331.1 $[M+H]^+$; elemental analysis calcd (%) for $C_{91}H_{143}NO_5$: C 82.11, H 10.83, N 1.05; found: C 82.67, H 11.07, N 1.02.

General procedure for the formation of the ammonium salt monomers: A solution of the amino precursor **1** (100 mg in 10 mL of $CHCl_3$; *care was taken to use HCl-free $CHCl_3$*) was gently shaken with 10 mL of the pertinent acid solution (1 M HCl/H_2O for **1**·HCl, 1 M DCl/D_2O for **1**·DCl, 1 M HBr/H_2O for **1**·HBr, and 1% picric acid in H_2O for **1**·HPic). The organic layer was separated from the aqueous one, washed twice with H_2O (5 mL; D_2O in the case of **1**·DCl), dried ($MgSO_4$) and concentrated to dryness under reduced pressure. The solid residue obtained was kept under high vacuum (2 h, RT) and each sample used as such to prepare the relevant stock solutions. CD_2Cl_2 (or CH_2Cl_2) was dispensed out of a freshly-opened bottle and passed through neutral alumina prior to use.

Acknowledgements

We thank Prof. M. Triscari and Dr. G. Sabatino (Università di Messina) for SEM measurements, Dr. D. Garozzo (CNR, ICTP Catania) for mass spectra, and Prof. G. Malandrino (Università di Catania) for useful discussions. We are also grateful to MiUR (PRIN-2006 project) for financial support of this work.

[1] a) *Supramolecular Polymers* 2nd ed. (Ed.: A. Ciferri), CRC Press, Boca Raton, FL, **2005**; b) L. Brunsveld, B. J. B. Folmer, E. W. Meijer, R. P. Sijbesma, *Chem. Rev.* **2001**, *101*, 4071–4097; c) J.-M. Lehn, *Polym. Int.* **2002**, *51*, 825–839; d) A. W. Bosman, L. Brunsveld, B. J. B. Folmer, R. P. Sijbesma, E. W. Meijer, *Macromol. Symp.* **2003**, *201*, 143–154; e) H. Hofmeister, U. S. Schubert, *Chem. Commun.* **2005**, 2423–2432.

[2] a) C. Fouquey, J.-M. Lehn, A.-M. Levelut, *Adv. Mater.* **1990**, *2*, 254–257; b) M. Kotera, J.-M. Lehn, J.-P. Vigneron, *Tetrahedron* **1995**, *51*, 1953–1972.

[3] H. A. Klok, K. A. Joliffe, C. L. Schauer, L. J. Prins, J. P. Spatz, M. Möller, P. Timmerman, D. N. Reinhoudt, *J. Am. Chem. Soc.* **1999**, *121*, 7154–7155.

[4] E. Kolomiets, J.-M. Lehn, *Chem. Commun.* **2005**, 1519–1521.

[5] R. P. Sijbesma, F. H. Beijer, L. Brunsveld, B. J. B. Folmer, J. H. K. K. Hirschberg, R. F. M. Lange, J. K. L. Lowe, E. W. Meijer, *Science* **1997**, *278*, 1601–1604.

[6] a) R. K. Castellano, D. M. Rudkevich, J. Rebek, Jr., *Proc. Natl. Acad. Sci. USA* **1997**, *94*, 7132–7137; b) R. K. Castellano, J. Rebek, Jr., *J. Am. Chem. Soc.* **1998**, *120*, 3657–3663; c) R. K. Castellano, C. Nuckolls, S. H. Eichhorn, M. R. Wood, A. J. Lovinger, J. Rebek, Jr., *Angew. Chem.* **1999**, *111*, 2764–2768; *Angew. Chem. Int. Ed.* **1999**, *38*, 2603–2606; d) R. K. Castellano, R. Clark, S. L. Craig, C. Nuckolls, J. Rebek, Jr., *Proc. Natl. Acad. Sci. USA* **2000**, *97*, 12418–12421; e) H. Xu, S. P. Stampp, D. M. Rudkevich, *Org. Lett.* **2003**, *5*, 4583–4586.

[7] For a comprehensive discussion of liquid crystals obtained from stacked aromatic discotic molecules, see *Handbook of Liquid Crystals, Vol. 2B* (Eds.: D. Demus, J. Goodby, G. W. Gray, H. W. Spiess, V. Vill) Wiley-VCH, Weinheim, **1998**, , and references therein.

[8] a) G. Li, L. B. McGown, *Science* **1994**, *264*, 249–251; b) M. W. Hosseini, A. De Cian, *Chem. Commun.* **1998**, 727–733; c) Y. Liu, Z. Fan, H.-Y. Zhang, C.-H. Diao, *Org. Lett.* **2003**, *5*, 251–254.

[9] a) M. Miyauchi, A. Harada, *J. Am. Chem. Soc.* **2004**, *126*, 11418–11419; b) M. Miyauchi, T. Hoshino, H. Yamaguchi, S. Kamitori, A. Harada, *J. Am. Chem. Soc.* **2005**, *127*, 2034–2035; c) M. Miyauchi, T. Hoshino, H. Yamaguchi, A. Harada, *J. Am. Chem. Soc.* **2005**, *127*, 2984–2989.

[10] N. Yamaguchi, D. S. Nagvekar, H. W. Gibson, *Angew. Chem.* **1998**, *110*, 2518–2520; *Angew. Chem. Int. Ed.* **1998**, *37*, 2361–2364.

[11] a) P. R. Ashton, I. Baxter, S. J. Cantrill, M. C. T. Fyfe, P. T. Glink, J. F. Stoddart, A. J. P. White, D. J. Williams, *Angew. Chem.* **1998**, *110*, 1344–1347; *Angew. Chem. Int. Ed.* **1998**, *37*, 1294–1297; b) S. J. Rowan, S. J. Cantrill, J. F. Stoddart, A. J. P. White, D. J. Williams, *Org. Lett.* **2000**, *2*, 759–762; c) S. J. Cantrill, G. J. Youn, J. F. Stoddart, *J. Org. Chem.* **2001**, *66*, 6857–6872; d) S.-H. Chiu, S. J. Rowan, S. J. Cantrill, J. F. Stoddart, A. J. P. White, D. J. Williams, *Chem. Commun.* **2002**, 2948–2949. See also P. R. Ashton, I. W. Parsons, F. M. Raymo, J. F. Stoddart, A. J. P. White, D. J. Williams, *Angew. Chem.* **1998**, *110*, 2016–2019; *Angew. Chem. Int. Ed.* **1998**, *37*, 1913–1916; for earlier experiments on bipyridinium-linked aromatic crown ethers.

[12] a) N. Yamaguchi, H. W. Gibson, *Angew. Chem.* **1999**, *111*, 195–199; *Angew. Chem. Int. Ed.* **1999**, *38*, 143–147; b) H. W. Gibson, N. Yamaguchi, J. W. Jones, *J. Am. Chem. Soc.* **2003**, *125*, 3522–3533; c) F. Huang, H. W. Gibson, *Chem. Commun.* **2005**, 1696–1698.

[13] a) Y. Hasegawa, M. Miyauchi, Y. Takashima, H. Yamaguchi, A. Harada, *Macromolecules* **2005**, *38*, 3724–3730; b) K. Ohga, Y. Takashima, H. Takahashi, Y. Kawaguchi, H. Yamaguchi, A. Harada, *Macromolecules* **2005**, *38*, 5897–5904.

[14] D. Garozzo, G. Gattuso, F. H. Kohnke, A. Notti, S. Pappalardo, M. F. Parisi, I. Pisagatti, A. J. P. White, D. J. Williams, *Org. Lett.* **2003**, *5*, 4025–4028.

[15] a) M. C. Jiménez, C. Dietrich-Buchecker, J. P. Sauvage, A. De Cian, *Angew. Chem.* **2000**, *112*, 1351–1354; *Angew. Chem. Int. Ed.* **2000**, *39*, 1295–1298; b) T. Hoshino, M. Miyauchi, Y. Kawaguchi, H. Yamaguchi, A. Harada, *J. Am. Chem. Soc.* **2002**, *124*, 9876–9877.

[16] S. Ishihara, S. Takeoka, *Tetrahedron Lett.* **2006**, *47*, 181–184.

[17] D. R. Stewart, D. C. Gutsche, *Org. Prep. Proc. Int.* **1993**, *25*, 137–139.

[18] *N*-(12-bromododecyl)phthalimide was prepared by a modification of a literature procedure. See: M. J. Pfammatter, V. Siljegovic, T. Darbre, R. Keese, *Helv. Chim. Acta* **2001**, *84*, 678–689.

[19] D. R. Stewart, M. Krawiec, R. P. Kashyap, W. H. Watson, C. D. Gutsche, *J. Am. Chem. Soc.* **1995**, *117*, 586–601.

[20] a) S. Pappalardo, M. F. Parisi, *J. Org. Chem.* **1996**, *61*, 8724–8725; b) F. Arnaud-Neu, S. Fuangswasdi, A. Notti, S. Pappalardo, M. F. Parisi, *Angew. Chem.* **1998**, *110*, 120–122; *Angew. Chem. Int. Ed.* **1998**, *37*, 112–114; c) M. Gattuso, A. Notti, S. Pappalardo, M. F. Parisi, *Tetrahedron Lett.* **1998**, *39*, 1965–1968.

[21] The presence of free monomeric species cannot be ruled out by ^{1}H NMR. In fact the diffusion NMR data did show that some unthreaded monomeric species are indeed present in the solution.

[22] Assignments reported in Figure 1b follow from a ^{1}H–^{1}H COSY experiment (see the Supporting Information).

[23] For additional examples of *endo*-cavity inclusion of alkylammonium and alkyldiammonium ions into calix[5]arene derivatives, see: a) G. Cafeo, G. Gattuso, F. H. Kohnke, A. Notti, S. Occhipinti, S. Pappalardo, M. F. Parisi, *Angew. Chem.* **2002**, *114*, 2226–2230; *Angew. Chem. Int. Ed.* **2002**, *41*, 2122–2126; b) D. Garozzo, G. Gattuso, F. H. Kohnke, P. Malvagna, A. Notti, S. Occhipinti, S. Pappalardo,

M. F. Parisi, I. Pisagatti, *Tetrahedron Lett.* **2002**, *43*, 7663–7667; c) F. P. Ballistreri, A. Notti, S. Pappalardo, M. F. Parisi, I. Pisagatti, *Org. Lett.* **2003**, *5*, 1071–1074; d) D. Garozzo, G. Gattuso, A. Notti, A. Pappalardo, S. Pappalardo, M. F. Parisi, M. Perez, I. Pisagatti, *Angew. Chem.* **2005**, *117*, 4970–4974; *Angew. Chem. Int. Ed.* **2005**, *44*, 4892–4896.

[24] The dodecylammonium alkyl chain is far too short to bend alongside the aromatic unit, fold over the *tert*-butyl group and reach the interior of the calixarene cavity, while access of the ammonium group from the lower rim is judged unlikely because this would imply curling of the alkyl chain back on itself with subsequent leaning of one of the aryl rings toward the cavity to relieve steric hindrance. In this event, however, the loss of symmetry of the cavity would have been detected by ^{1}H NMR spectroscopy. See: G. De Salvo, G. Gattuso, A. Notti, M. F. Parisi, S. Pappalardo, *J. Org. Chem.* **2002**, *67*, 684–692.

[25] For self-threading of a poly(ethylene glycol) chain in cyclodextrins, see: Y. Inoue, M. Miyauchi, H. Nakajima, Y. Takashima, H. Yamaguchi, A. Harada, *J. Am. Chem. Soc.* **2006**, *128*, 8994–8995.

[26] a) P. J. Flory, *Principles of Polymer Chemistry*, Cornell University Press, Cornell, **1953**, p. 317–346; b) U. Michelsen, C. A. Hunter, *Angew. Chem.* **2000**, *112*, 780–783; *Angew. Chem. Int. Ed.* **2000**, *39*, 764–767; c) W. Knoben, N. A. M. Besseling, M. A. Cohen Stuart, *Macromolecules* **2006**, *39*, 2643–2653.

[27] The iterative inclusion of **1**·HX was assumed to be isodesmic (R. B. Martin, *Chem. Rev.* **1996**, *96*, 3043–3064). The number-average degree of polymerization was calculated by the Carothers equation (C. H. Carothers, *Trans. Faraday Soc.* **1936**, *32*, 39–49), $\bar{X}_n = 1/(1-p)$, where p is the fraction of complexed species. This expression assumes that cyclic species are not present in significant amounts.

[28] a) S. Bartoli, S. Roelens, *J. Am. Chem. Soc.* **1999**, *121*, 11908–11909; b) V. Böhmer, A. Dalla Cort, L. Mandolini, *J. Org. Chem.* **2001**, *66*, 1900–1902; c) A. Arduini, E. Brindani, G. Giorgi, A. Pochini, A. Secchi, *J. Org. Chem.* **2002**, *67*, 6188–6194; d) J. W. Jones, H. W. Gibson, *J. Am. Chem. Soc.* **2003**, *125*, 7001–7004; e) F Huang, J. W. Jones, C. Slebodnik, H. W. Gibson, *J. Am. Chem. Soc.* **2003**, *125*, 14458–14464; f) M. Clemente-León, C. Pasquini, V. Hebbe-Viton, J. Lacour, A. Dalla Cort, A. Credi. *Eur. J. Org. Chem.* **2006**, 105–112.

[29] For reviews on the application of diffusion NMR in chemical systems, see: a) P. Stilbs, *Prog. Nucl. Magn. Reson. Spectrosc.* **1987**, *19*, 1–45; b) C. S. Johnson, Jr., *Prog. NMR Spectrosc.* **1999**, *34*, 203–256.

[30] For recent applications of diffusion NMR in supramolecular chemistry, see: a) O. Mayzel, Y. Cohen, *J. Chem. Soc. Chem. Commun.* **1994**, 1901–1902; b) O. Mayzel, O. Aleksiuk, F. Grynszpan, S. E. Biali, Y. Cohen, *J. Chem. Soc. Chem. Commun.* **1995**, 1183–1184; c) A. Gafni, Y. Cohen, *J. Org. Chem.* **1997**, *62*, 120–125; d) L. Frish, S. E. Matthews, V. Böhmer, Y. Cohen, *J. Chem. Soc. Perkin Trans. 2* **1999**, 669–671; e) L. Avram, Y. Cohen, *J. Am. Chem. Soc.* **2002**, *124*, 15148–15149; f) L. Avram, Y. Cohen, *J. Am. Chem. Soc.* **2004**, *126*, 11556–11563; g) M. Tominaga, K. Suzuki, M. Kawano, T. Kusukawa, T. Ozeki, S. Sakamoto, K. Yamaguchi, M. Fujita, *Angew. Chem.* **2004**, *116*, 5739–5743; *Angew. Chem. Int. Ed.* **2004**, *43*, 5621–5625; h) N. Kuhnert, A. Le-Gresley, *Org. Biomol. Chem.* **2005**, *3*, 2175–2182; i) M. S. Kaucher, Y.-F. Lam, S. Pieraccini, G. Gottarelli, J. T. Davis, *Chem. Eur. J.* **2005**, *11*, 164–173; j) Y. Cohen, L. Avram, L. Frish, *Angew. Chem.* **2005**, *117*, 524–560; *Angew. Chem. Int. Ed.* **2005**, *44*, 520–554.

[31] Oligomerization was directly carried out in the NMR tube by adding 4 μL of 20% DCl in D_2O to 300 μL of the CD_2Cl_2 solution of **1**.

[32] a) G. Ercolani, L. Mandolini, P. Mencarelli, S. Roelens, *J. Am. Chem. Soc.* **1993**, *115*, 3901–3908; b) A. T. ten Cate, H. Kooijman, A. L. Spek, R. P. Sijbesma, E. W. Meijer, *J. Am. Chem. Soc.* **2004**, *126*, 3801–3808.

[33] A. Wong, R. Ida, L. Spinder, G. Wu, *J. Am. Chem. Soc.* **2005**, *127*, 6990–6998. The model is based on the work of: M. M. Triado, C. Lopez Martinez, J. Garcia de la Torre, *J. Chem. Phys.* **1984**, *81*, 2047–2052.

[34] H.-J. Schneider, R. Kramer, S. Simova, U. Schneider, *J. Am. Chem. Soc.* **1988**, *110*, 6442–6448.

[35] When solutions of **1**·DCl (prepared as described in the "Experimental Section" under the sub-heading "General procedure for the formation of the ammonium salt monomers") in D_2O-free CD_2Cl_2 (dispensed out of a freshly-opened bottle) were used, the diffusion coefficients (Table 2) were consistently found to be slightly higher than those observed for **1**·DCl obtained by *in situ* addition of DCl/D_2O (see ref. [31]). Furthermore, under these conditions, ^{1}H NMR integration (data not shown) displayed an average decrease ($\approx$6%) in the percentages of threading. These observations indicate that in the absence of D_2O, both the lack of ion solvation and greater extent of ion-pairing result in a modest but detectable decrease in the self-assembly.

[36] F. Hofmeister, *Arch. Exp. Pathol. Pharmakol.* **1888**, *24*, 247–260.

[37] P. S. Pregosin, *Prog. NMR Spectrosc.* **2006**, *49*, 261–288.

[38] a) B. Chu, *Light Scattering, Basic Principles and Practice*, Academic, San Diego, **1991**; b) *Light Scattering: Principles and Development* (Ed.: W. Brown), Clarendon, Oxford, **1996**.

[39] B. J. Berne, R. Pecora, *Dynamic Light Scattering with Applications to Chemistry, Biology and Physics*, Wiley, New York, **1976**.

[40] D. Lombardo, N. Micali, V. Villari, *Phys. Rev. E* **2004**, *70*, 21402.

[41] C. A. Schalley, *Mass Spectrom. Rev.* **2001**, *20*, 253–309.

[42] D. D. Perrin, W. L. F. Armarego, *Purification of Laboratory Chemicals*, Pergamon Press, Oxford, **1989**.

[43] S. J. Gibbs, C. S. Johnson Jr. , *J. Magn. Reson.* **1991**, *93*, 395–402.

[44] a) M. Corti, V. Degiorgio, *Phys. Rev. Lett.* **1980**, *45*, 1045–1048; b) M. Corti, V. Degiorgio, *J. Phys. Chem.* **1981**, *85*, 711–717.

[45] P. Stepanek in *Dynamic Light Scattering: The Method and Some Applications*, (Ed.: W. Brown), Clarendon, Oxford, **1993**, p. 177.

Received: December 13, 2006
Revised: April 27, 2007
Published online: July 17, 2007

